

Reconfiguration of B-DNA structure induced by ethanol

Yue Huang(黄悦), Yipeng Chen(陈以鹏), Jing Li(李静), Rongri Tan(谈荣日), and Huanhuan Qiu(邱环环)
Citation: Chin. Phys. B, 2025, 34 (**8**): 088707. DOI: 10.1088/1674-1056/adbed9
http://cpb.iphy.ac.cn; http://iopscience.iop.org/cpb

What follows is a list of articles you may be interested in

Heterogeneous hydration patterns of G-quadruplex DNA

Cong-Min Ji(祭聪敏), Yusong Tu(涂育松), and Yuan-Yan Wu(吴园燕)
Chin. Phys. B, 2023, 32 (**2**): 028702. DOI: 10.1088/1674-1056/ac7452

Coarse-grained simulations on interactions between spectrins and phase-separated lipid bilayers

Xuegui Lin(林雪桂), Xiaojie Chen(陈晓洁), and Qing Liang(梁清)
Chin. Phys. B, 2021, 30 (**6**): 068701. DOI: 10.1088/1674-1056/abf129

Tail-structure regulated phase behaviors of a lipid bilayer

Wenwen Li(李文文), Zhao Lin(林召), Bing Yuan(元冰), and Kai Yang(杨恺)\ccclink
Chin. Phys. B, 2020, 29 (**12**): 128701. DOI: 10.1088/1674-1056/abad20

Effects of Mg^{2+} on the binding of the CREB/CRE complex: Full-atom molecular dynamics simulations

Song Mao(毛松), Shuai Wang(王帅), Haiyou Deng(邓海游), Ming Yi(易鸣)
Chin. Phys. B, 2019, 28 (**7**): 078701. DOI: 10.1088/1674-1056/28/7/078701

Molecular dynamic simulation of the thermodynamic and kinetic properties of nucleotide base pair

Yu-Jie Wang(王宇杰), Zhen Wang(王珍), Yan-Li Wang(王晏莉), Wen-Bing Zhang(张文炳)
Chin. Phys. B, 2017, 26 (**12**): 128705. DOI: 10.1088/1674-1056/26/12/128705

SPECIAL TOPIC — A celebration of the 90th Anniversary of the Birth of Bolin Hao

Reconfiguration of B-DNA structure induced by ethanol

Yue Huang(黄悦)[†], Yipeng Chen(陈以鹏)[†], Jing Li(李静), Rongri Tan(谈荣日)[‡], and Huanhuan Qiu(邱环环)[§]

Department of Physics, Jiangxi Science and Technology Normal University, Nanchang 330038, *China*

(Received 11 November 2024; revised manuscript received 13 February 2025; accepted manuscript online 11 March 2025)

Solution environment can influence the flexible structure of DNA under specific conditions, thereby affecting the stability of nucleic acids and ultimately impacting critical biological processes such as replication and transcription. Intracellular solution environment is variable, and previous studies have demonstrated that it can enhance the stability of DNA structures under certain circumstances. In this work, molecular dynamics simulations were conducted on B-DNA (1ZEW, with a nucleotide sequence of CCTCTAGAGG) derived from human breast cancer cells (MDA-MB231) to explore the effects of ethanol solution on DNA configuration transformation at different temperatures and concentrations. The calculated results indicate that ethanol facilitates the transition of 1ZEW from B-DNA to A-DNA at lower temperature. Furthermore, it is observed that temperature affects DNA structure to some extent, thereby modifying the trend in DNA configuration transformation. At low temperatures, the ethanol can promote the transformation of B-DNA into A-DNA at higher concentrations. While at higher temperatures, the DNA could be in a state of thermal melting. These conclusions presented here can give valuable insights into how ethanol affects B-DNA configuration transformations.

Keywords: ethanol, molecular dynamic simulation, DNA configuration

PACS: 87.14.gk, 87.15.ap, 87.15.–v, 87.15.hp

DOI: 10.1088/1674-1056/adbed9 **CSTR:** 32038.14.CPB.adbed9

1. Introduction

The human cell environment is a complex and diverse intracellular milieu characterized by the presence of a wide range of small ions, organic compounds, and other biomolecules.[1–3] The solution environment constitutes a significant portion of the cytoplasmic and endonuclear volumes, influencing the flexible structure of DNA in various ways.[4,5] On one hand, they can enhance the stability of DNA structure, while on the other hand, they can also promote the transition of DNA configuration, altering the stability of nucleic acids and impacting crucial biological processes like DNA replication and transcription.[6,7] Moreover, changes in DNA structure can lead to many diseases.[8,9] Therefore, understanding the effects of solution environment on DNA is essential for further research in pharmaceutics and medical sciences.[10–12]

Experimental studies have indeed investigated the impact of solution environment on DNA. Lai *et al.* found that aggregation of DNA was necessary to form A-DNA through changes in the solution.[13] Yao *et al.* used the nanopore single-molecule analytical technique to demonstrate that the event frequency and translocation time increase with the increase of crowding concentration, indicating a non-monotonic dependence on the size of the crowding molecules.[14] Ghosh *et al.* proposed a method for predicting the stability of short DNA duplexes in various cosolutes and determined nearest-neighbor parameters for DNA duplex formation under similar solution conditions.[15] Furthermore, Shet *et al.* presented B-DNA as a biomacromolecular crowding system and found that the presence of various concentrations of B-DNA from salmon milt resulted in an 11-fold higher catalytic activity. These experimental studies provide valuable insights into the effects of molecular crowding on DNA and contribute to our understanding of how crowding molecules influence the structure and function of DNA in complex cellular environments.[16] Additionally, Deng *et al.* studied Mtb DNA gyrase under macromolecular crowding conditions by incorporating PEGs and PVAs into the DNA supercoiling reactions. They discovered that high concentrations of potassium glutamate, glycine betaine, PEGs, and PVA substantially stimulated the DNA supercoiling activity of Mtb DNA gyrase. These findings further highlight the importance of considering molecular crowding in understanding the behavior and function of DNA in cellular environments.[17]

Theoretical studies have also investigated the effects of solution environment on DNA. Kumar *et al.* examined the competition between glycol and water molecules by altering the molecular crowding in glycol solution and found that the ion density near DNA increased with the concentration of ethylene glycol.[18] Zhang *et al.* studied the influence of changing concentrations of ethylene glycol (EG) solution on

[†]These authors contributed equally to this work and should be considered co-first authors.

[‡]Corresponding author. E-mail: rogertanr@hotmail.com

[§]Corresponding author. E-mail: qiu.hhhh@126.com

© 2025 Chinese Physical Society and IOP Publishing Ltd. All rights, including for text and data mining, AI training, and similar technologies, are reserved.

the polymorphism and flexibility of B-DNA, concluding that a high concentration of EG promotes structural stability.[19] Shim *et al*. employed a three-pronged, systems-molecular approach to capture dynamic crowding and investigate its influence on transcription.[20] Khoshbin *et al*. used MD simulations to study the influence of temperature and molecular crowding on the sensitivity of the T30695 aptamer towards Pb^{2+}, finding that the aptamer is most sensitive in a solution with a 5% v/v concentration of ethanol.[21] Hong *et al*. used a coarse-grained model of DNA to investigate the kinetics and thermodynamics of DNA duplex and hairpin formation in crowded environments, discovering that crowders can elevate the melting temperature of DNA structures depending on the excluded volume fraction and size of the crowder.[22]

Most of the previous experimental investigations employed inert molecules such as ethylene glycol, polyethylene glycol and so on. While the theoretical researches in the past decades mainly focused on the effect of dielectric constant of ethanol, the effect of ethanol solution on DNA configuration should be investigated. In this work, molecular dynamics simulations were carried out to investigate the crowding effect of ethanol solutions on the transition of DNA configuration in human breast cancer cells at different concentrations and temperatures. The axial base and groove feature parameters were calculated using the curves+ and 3DNA program to investigate the changing trend of DNA configuration. Moreover, the hydrogen bonds and radial distribution function (RDF) were calculated to analyze how ethanol affects the transition of DNA configurations. In addition, we also computed the melting temperature by using the DINAMelt server program to analyze the possible DNA melting transition at 320 K. We firmly believe that this work can give valuable insights into how ethanol affects B-DNA configuration transformations.

2. Computational methods

Based on our research experiences on the structural stability of A-DNA in the salt solution of different concentrations using molecular dynamics simulations,[23,24] three different solvent systems consist of water and ethanol, whose volume concentrations are respectively 40%, 60% and 80%, were designed to study the conformational transitions of a double-stranded B-DNA at different temperatures (280 K, 300 K, and 320 K). The B-DNA with a nucleotide sequence of CCTCTAGAGG is from human breast cancer cells,[25–27] which is called 1ZEW in the Protein Data Bank. The size of simulation cubic box including a DNA, ethanol, SPC water molecules[28] and Na^+ ions is 60 Å×60 Å×60 Å, which is big enough to prevent the interaction between DNA itself and its periodic images.[29] Here, the Na^+ ions were added into the system to make sure the solution environment is electrically neutral.

All the simulations were performed using the GROMACS 5.1.5 program with the AMBER99SB force field.[30,31] To avoid cutoff effects, long range electrostatic interactions were calculated by the particle mesh Ewald summation method.[32] All simulations are conducted at a constant pressure of 1 bar, which are also implemented at different constant temperatures (280 K, 300 K, and 320 K). Each simulation process lasts 200 nanoseconds with a time step of 2 femtoseconds. The simulation of molecular dynamics involves four key steps. Initially, energy minimization techniques are employed to ensure there are no spatial collisions or improper geometric configurations in the system. Subsequently, NVT equilibration is performed to stabilize the temperature at the desired value. Additionally, pressure equilibration is achieved under an NPT ensemble. Finally, an MD simulation equilibrium is run for 200 ns to obtain the final structure for analysis.

After simulation, the DNA groove properties and axial base parameters were analyzed using the curves+ program.[33] For comparison, the typical A-DNA and B-DNA structures with the same sequence of CCTCTAGAGG were also generated using the 3DNA program.[34] To analyze the DNA melting transition, the melting temperature was computed by using the DINAMelt server program.[35]

3. Results and discussion

3.1. Axial base and groove feature parameters

The axial base[36] and groove feature parameters[37] are the most fundamental and crucial structural factors that determine the type of DNA. To distinguish and determine the conformation of DNA at room temperature 300 K, we calculated the axial base and groove parameters as a function of increasing ethanol concentration. The axial base parameters encompass the base pair helix, step length parameters and the type of base pair sugar puckers. Specifically, the base pair helix parameters include vertical displacement (X-disp), inclination angle (Inclination), helical rise (H-rise), and helical twist (H-twist), as shown in Fig. 1. While the step length parameters consist of slide angle (Slide), roll angle (Roll), twist angle (Twist), and propeller angle (Propeller), as shown in Fig. 2. In addition, to ensure data reliability, we computed the mean and standard deviation of each parameter for the last 2 ns after the system reached equilibrium at 300 K. Then, we added error bar analysis to the axial base and groove characteristic parameters in ethanol solutions of varying concentrations at 300 K. From the error bar analysis, it can be seen clearly that the data fluctuate less, which indicates that the data are relatively reliable and true.

From Fig. 1(a), it can be seen clearly that the X-disp value decreases from −1.6 Å to −3.24 Å when the concentration of ethanol increases from 40% to 80%, gradually approaching the

typical A-form DNA structure. For comparative analysis, we incorporated the DNA structural parameters obtained in pure water as a reference. The simulation data reveal that within ethanol concentrations below 40% (v/v), the X-disp values exhibit minimal variation, demonstrating only a marginal decrease from −1.57 Å to −1.60 Å. The variation trends of the H-rise and H-twist values on the surface of Figs. 1(c) and 1(d) are similar to those of X-disp. With the increase of concentration, the H-rise distance and the H-twist angle decrease from 3.39 Å to 3.06 Å and 32.6° to 27.8°, respectively. Furthermore, within the concentration range of 0 to 40%, both parameters exhibit minimal variation, showing only slight decreases from 3.42 Å to 3.39 Å and from 33.8° to 22.6°, respectively. However, it can be seen from the data in Fig. 1(b) that with the increase of concentration, the angle of inclination gradually increases from 3° to 8.9°. The variation in the inclination angle demonstrates consistency with other measured parameters across the concentration range of 0 to 40%, showing a gradual increase from 2.6° to 3.0° without statistically significant changes.

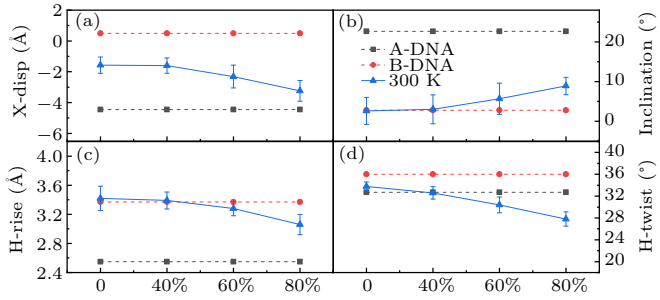


Fig. 1. The average value of DNA base pair helix parameters at 300 K in pure water and ethanol with the respective concentrations of 40%, 60%, and 80%. (a) X-displacement (X-disp), (b) inclination angle (Inclination), (c) helical rise (H-rise), and (d) helical twist (H-twist). For comparison, the reference values for typical A-DNA (grey, square) and B-DNA (red, circle) are given. The error bars (blue, T-shaped sign) are also marked in the figure.

It is obvious in Fig. 2(a) that the value of slide decreases from −0.75 Å to −1.39 Å with the concentration of ethanol increasing from 40% to 80%, and the trend of change in the twist angle as shown in Fig. 2(c) is similar to the slide, which the angle of twist goes down from 32.7° to 27.5° with the increase of concentration. And as the concentration is below 40%, the slide decreases from −0.56 Å to −0.75 Å while the twist is still 32.7°. From Fig. 2(b), we can see that when the concentration increases from 0 to 40%, the roll value increases from 1.1° to 1.8°. When the ethanol concentration further increases to 80%, the roll value increases from 1.8° to 4.1°. It can also be learned from Fig. 2(d) that the trend of change in the propeller is similar to that of roll, which rises from −12° to −7.8° as the increase of solvent concentration. when the concentration increases from 0 to 40%, the propeller value rises from −16.7° to −12°. From the data above, we can learn that when the temperature is 300 K, the DNA structure didn't change much in lower concentration within the range of 0 to 40%, while in high concentration of ethanol from 40% to 80%, the final structure of the DNA exhibits features of an irregular A-form. Therefore, at 300 K, higher concentrations of ethanol favor the transition from B-DNA to A-DNA.

To further confirm this, we analyzed the type of base pair sugar puckers at 300 K as shown in Table 1, where the structural data of original 1ZEW, typical A-DNA and B-DNA are given for comparison. It can be seen clearly from the Table 1 that the sugar puckers in typical B-DNA are predominantly C2′-endo whereas they are primarily C3′-endo in typical A-DNA, and the structure of the original 1ZEW is B-DNA. In addition, when the concentration of the ethanol solution reaches 80%, the proportion of C2′-endo significantly decreases, with most sugar puckers transitioning to C1′-exo and C3′-endo, confirming the transformation of 1ZEW into an irregular A-form.

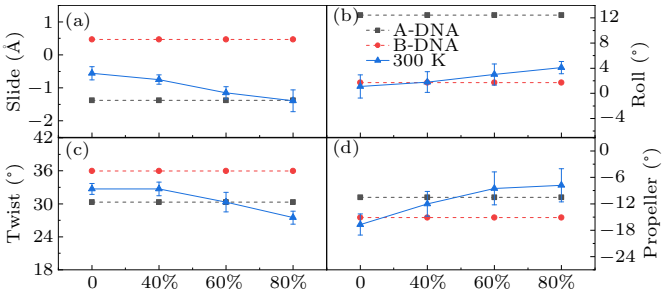


Fig. 2. The average value of DNA step length parameters at 300 K in pure water and ethanol with the respective concentrations of 40%, 60%, and 80%. (a) Sliding angle (Slide), (b) rolling angle (Roll), (c) twist angle (Twist) between base pairs, and (d) the internal deflection angle of the base pairs (Propeller). For comparison, the reference values for typical A-DNA (grey, square) and B-DNA (red, circle) are given. The error bars (blue, T-shaped sign) are also marked in the figure.

It is well established that DNA grooves consist of minor and major grooves. To further investigate the effect of ethanol on DNA structure, major and minor groove widths were calculated using the method developed by Hassan and Calladine.[38] This method calculates cross-strand P–P distances considering the direction of the sugar-phosphate backbone. Figure 3(a) shows that with the increase in ethanol concentration to 40%, the width of the minor groove expands from 12.2 Å to 13.9 Å compared to typical B-type DNA. In the lower concentration range, the width of the minor groove increases from 12.9 Å to 13.9 Å when the concentration rises from 0 to 40%. Furthermore, as the concentration of ethanol is increased from 40% to 80%, a more extensive widening of the minor groove is observed, reaching 16.1 Å and gradually approaching the 18.3 Å observed in typical A-type DNA. Compared with the minor groove width, the major groove width shown in Fig. 3(b) also widens. As the concentration ranges from 0 to 40%, the major groove width widens from 6.1 Å to 10.8 Å. When the concentration increases to 80%, the major groove width further increases to 15.8 Å, which is closer to that of the typical A-type DNA.

Table 1. The base pair sugar pucker of the typical A-DNA, typical B-DNA, original 1ZEW and 1ZEW in different ethanol concentrations (40%, 60%, and 80%) at 300 K.

Typical A-DNA		Typical B-DNA		Original 1ZEW		300 K					
						40%		60%		80%	
Strand I	Strand II	Strand I	Strand II	Strand I	Strand II	Strand I	Strand II	Strand I	Strand II	Strand I	Strand II
C3′-endo	C3′-endo	C2′-endo	C1′-exo	C2′-endo	C2′-endo	O1′en	C1′ex	O1′en	C2′en	O1′en	C1′ex
C3′-endo	C3′-endo	C2′-endo	C1′-exo	C2′-endo	C2′-endo	C2′en	C1′ex	C2′en	C2′en	C1′ex	C2′en
C3′-endo	C3′-endo	C2′-endo	C1′-exo	C2′-endo	C3′-exo	O1′en	C1′ex	C1′ex	C2′en	C1′ex	C2′en
C3′-endo	C3′-endo	C2′-endo	C1′-exo	C2′-endo	C3′-exo	C2′en	C2′en	C1′ex	C3′ex	O1′en	C1′ex
C3′-endo	C3′-endo	C1′-exo	C1′-exo	C2′-endo	C2′-endo	C2′en	C2′en	O1′en	C1′ex	C1′ex	C1′ex
C3′-endo	C3′-endo	C1′-exo	C1′-exo	C2′-endo	C2′-endo	C1′ex	C1′ex	C2′en	C2′en	C1′ex	C1′ex
C3′-endo	C3′-endo	C1′-exo	C2′-endo	C2′-endo	C2′-endo	C1′ex	C2′en	C2′en	O1′en	C3′ex	C1′ex
C3′-endo	C3′-endo	C1′-exo	C2′-endo	C2′-endo	C2′-endo	C3′ex	C1′ex	O1′en	C3′en	C1′ex	O1′en
C3′-endo	C3′-endo	C1′-exo	C2′-endo	C2′-endo	C3′-exo	O1′en	C2′en	C2′en	O1′en	C2′en	O1′en
C3′-endo	C3′-endo	C1′-exo	C2′-endo	C2′-endo	C2′-endo	C1′ex	C1′ex	C2′en	O1′en	C1′ex	C3′en

It is noteworthy that we have observed deviations of 1ZEW from the typical B-DNA structure typically found in pure water. To ascertain the underlying causes of these deviations, we further analyzed the root-mean-square fluctuations (RMSF) of DNA at 280 K and 300 K, which are shown in Fig. S1. It can be seen clearly that the RMSF values of DNA chain in pure water are almost 2.07 nm at 300 K, while the RMSF values of DNA chain at 280 K are between 2.14 nm and 2.19 nm in pure water, which are much larger than the values at 300 K. What's more, when at 300 K, there are huge distortions in the structure of DNA chains. The changing part is located at atoms from 283 to 316 and atoms from 317 to 344, which are derived from base 10 DG and base 11 DC, respectively. In that case, it can be learned that the structural changes of DNA tend to happen at the ends of DNA chains, rather than the center part. Based on the data analysis, it can be inferred that the structural changes happened at the ends of DNA chains contribute to the deviation of axial base and groove feature parameters in 1ZEW from those parameters of typical B-DNA in pure water.

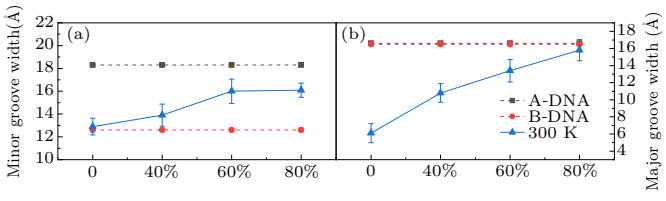


Fig. 3. At 300 K, the width of (a) the minor and (b) major grooves in pure water and ethanol with the respective concentrations of 40%, 60%, and 80%. For comparison, the reference values for typical A-DNA (grey, square) and B-DNA (red, circle) are given. The error bars (blue, T-shaped sign) are also marked in the figure.

In general, it can be concluded that when at a concentration of 80%, the final DNA structure most closely resembles the A-form DNA structure. This indicates that the solution environment drives the transition from B-DNA to A-DNA, with structural properties changing in response to increasing ethanol concentration. These results align with previous study which proved from the view of free-energy that the configuration of 1ZF1 is transferred from B-DNA to A-DNA when the concentration reaches 40%.[39] Additionally, data from lower ethanol concentrations ranging from 0 to 40% indicate that B-DNA is more stable in water than in ethanol solutions.

To further examine the impact of temperature on DNA configuration, the corresponding parameters above were renewed at the temperature of 280 K and 320 K, as shown in Figs. 4–6 and Table 2. It can be observed clearly from Figs. 4 and 5 that the change pattern of all parameters (X-disp, Inclination, H-rise, H-twist, Slide, Roll, Twist and Propeller) with concentration is almost the same at 280 K and 300 K, while the change pattern at 320 K is opposite. The structure parameters for the DNA in the ethanol solution with the concentrations of 40%, 60% and 80% at 320 K were obtained within the last 1 ns before the two ssDNA strands separate, and we selected 10 DNA structures during the 1 ns.

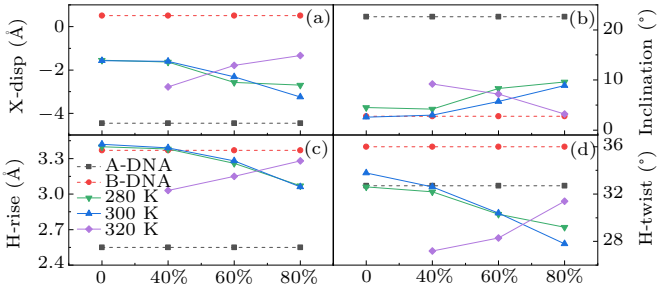


Fig. 4. The average value of DNA structure parameters at 280 K, 300 K, and 320 K in pure water and ethanol with the respective concentrations of 40%, 60%, and 80%. (a) X-displacement (X-disp), (b) inclination angle (Inclination), (c) helical rise (H-rise), and (d) helical twist (H-twist). For comparison, the reference values for typical A-DNA (grey, square) and B-DNA (red, circle) are given.

Here, the emphasis is placed on the situation at 320 K. As shown in Fig. 4(a), the X-disp value increases from −2.78 Å to −1.33 Å at 320 K with the increase of concentration, and the changing trend of the H-rise and H-twist value shown in Figs. 4(c) and 4(d) is similar to that of X-disp, where the distance of H-rise rises from 3.03 Å to 3.28 Å and the angle of H-twist goes up from 27.2° to 31.4° at 320 K as the concentration of ethanol increases from 40% to 80%. However, we can learn from the data in Fig. 4(b) that the inclination value

decreases from 9.2° to 3.2° at 320 K as the concentration increases.

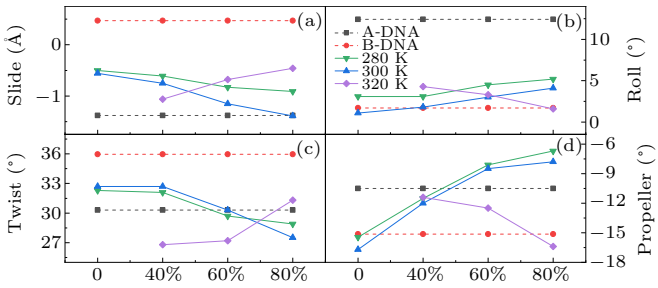


Fig. 5. The average value of DNA structure parameters at 280 K, 300 K, and 320 K in pure water and ethanol with the respective concentrations of 40%, 60%, and 80%. (a) Sliding angle (Slide), (b) rolling angle (Roll), (c) twist angle (Twist) between base pairs, and (d) the internal deflection angle of the base pairs (Propeller). For comparison, the reference values for typical A-DNA (grey, square) and B-DNA (red, circle) are given.

It can be learned from Fig. 5(a) that the value of slide increases from −1.06 Å to −0.46 Å with the ethanol concentration increasing from 40% to 80%, and the trend of change in the twist angle as shown in Fig. 5(c) is similar to the slide, which the angle of twist rises from 26.8° to 31.3° with the increase of the concentration. However, the roll value decreases from 4.3° to 1.6° at 320 K when the concentration increases from 40% to 80% as shown in Fig. 5(b). What is more, it can be learned from the data shown in Fig. 5(d) that the changing trend of propeller is similar to that of roll, which declines from −11.4° to −16.4° at 320 K as the concentration increases from 40% to 80%. In that case, it can be conclude from these results that when the temperature is below 320 K, the increase in ethanol concentration accelerates the transformation of 1ZEW into A-DNA, while the opposite phenomenon is observed when the temperature rises to 320 K.

The types of sugar pucker at 280 K and 320 K are shown in Table 2, it can be seen clearly that when at 280 K, the amount of C2′-endo decreases while the amount of C1′-exo increases when the ethanol concentration ranges from 40% to 80%. Conversely, at 320 K, as the concentration increases from 40% to 80%, the amount of C2′-endo increases while C1′-exo decreases, opposite to the trend at 280 K.

Table 2. The base pair sugar pucker of 1ZEW in different ethanol concentrations (40%, 60%, and 80%) at 280 K and 320 K.

280 K						320 K					
40%		60%		80%		40%		60%		80%	
Strand I	Strand II	Strand I	Strand II	Strand I	Strand II	Strand I	Strand II	Strand I	Strand II	Strand I	Strand II
O1′en	C1′ex	C1′ex	O1′en	C1′ex	C1′ex	C4′ex	C1′ex	C2′en	C1′ex	C1′ex	C3′en
C1′ex	C2′en	C2′en	C2′en	C2′en	C1′ex	C2′en	C1′ex	C2′en	C2′en	C2′en	C2′en
C4′ex	C2′en	O1′en	C2′en	O1′en	C1′ex	C2′en	O1′en	C1′ex	C2′en	C1′ex	O1′en
O1′en	C2′en	C2′en	C1′ex	C1′ex	C1′ex	O1′en	C1′ex	O1′en	C2′en	O1′en	C1′ex
C2′en	C1′ex	O1′en	C1′ex	C1′ex	C1′ex	C2′en	C2′en	O1′en	C1′ex	C1′ex	C2′en
C1′ex	C1′ex	C1′ex	C1′ex	C1′ex	C1′ex	C1′ex	C1′ex	O1′en	C1′ex	C1′ex	C1′ex
C1′ex	C2′en	C2′en	C1′ex	C1′ex	C1′ex	C2′en	O1′en	C1′ex	C1′ex	C1′ex	C1′ex
C2′en	O1′en	C1′ex	C1′ex	C2′en	C1′ex	C2′en	O1′en	C2′en	C3′en	O1′en	C2′en
C1′ex	O1′en	O1′en	C1′ex	C2′en	C2′en	C2′en	O1′en	O1′en	C2′en	C3′ex	C1′ex
C1′ex	C2′en	C1′ex	C2′en	C2′en	C3′en	C2′en	C2′en	C1′ex	C2′en	C2′en	C2′en

Upon examining Fig. 6(a), it is evident that the width of the minor groove decreases from 17.14 Å to 15.83 Å with an increase in the concentration from 40% to 80% at 320 K. Meanwhile, as illustrated in Fig. 6(b), the width of the major groove undergoes a reduction from 16.55 Å to 13.8 Å as the solvent concentration rises at the same temperature of 320 K. At a concentration of 80%, the discrepancy in width between the major and minor grooves amounts to 2.03 Å, deviating from the characteristic A-DNA width difference of 1.74 Å.

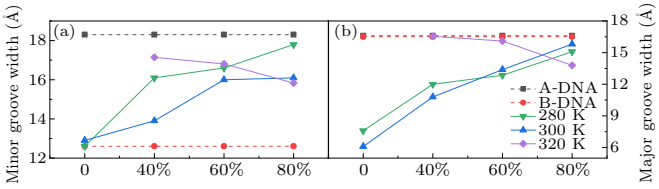


Fig. 6. At 280 K, 300 K, and 320 K, the width of (a) the minor and (b) major grooves in pure water and ethanol with the respective concentrations of 40%, 60%, and 80%. For comparison, the reference values for typical A-DNA (grey, square) and B-DNA (red, circle) are given.

Based on the quantitative analysis of the collected data, it can be conclusively demonstrated that under lower temperature conditions, ethanol facilitates the transition of B-DNA into A-DNA when exposed to higher concentrations. At higher temperatures, the structural modifications observed in 1ZEW appear to involve more complex conformational changes beyond a simple DNA configuration transition. To analyze the underlying mechanisms responsible for these differential behaviors, we conducted further systematic analysis at 320 K.

To elucidate the underlying mechanism responsible for the contrasting patterns observed at 320 K compared to 300 K, we investigated the potential DNA melting transition at 320 K. DNA melting transition generally refers to the process that double-stranded DNA is chemically or physically converted to single strands in vitro.[40] This transition mainly includes: thermal melting (heat), chemical melting (alkali, low ionic strength, organic solvents, chaotropes), mechanical melting

and electrophoretic melting. We found that the melting transition of 1ZEW at 320 K is the thermal melting, which is the most extensively studied and fundamental melting mechanism. During the process of thermal melting transition, the interactions between hydrogen bonds and base pairs in the DNA double strand gradually weaken, eventually leading to the separation of the double strand into a single strand. The temperature at which 50% of double-stranded DNA is converted to single-stranded DNA is referred to as the melting temperature (T_m) of that DNA.[41]

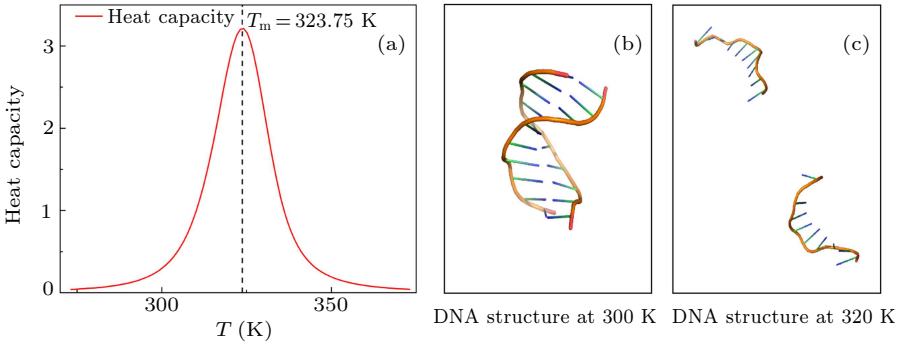


Fig. 7. (a) Heat capacity as a function of temperature; (b) and (c) DNA structure in pure water after simulations at different temperatures.

Therefore, we analyzed the specific melting temperature (T_m) of 1ZEW, which was calculated by numerically differentiating the collective free energy and plotted as a temperature function, as shown in Fig. 7(a). The maximum value was identified and marked as the melting temperature T_m. It can be learned from Fig. 7(a) that the maximum value occurs at 323.75 K, indicating that the T_m of 1ZEW is approximately 323.8 K. So when the temperature reaches 320 K, the DNA system approaches its melting transition state, thereby explaining the contrasting behavior observed at 320 K compared to 300 K. Moreover, the DNA structure in pure water after simulation is shown in Figs. 7(b) and 7(c). It can be learned that the double-stranded 1ZEW could be converted to single strands at 320 K.

3.2. Hydrogen bonds

The hydrogen bonds between water and DNA play a crucial role in the transformation of DNA configuration.[42] Moreover, hydrogen bonds serve as the primary force connecting the base pairs between the two strands of DNA, simultaneously stabilizing the double-helical structure of DNA.To quantitatively assess these interactions, we systematically investigated the concentration-dependent variation of hydrogen bond formation between water and DNA presented in Fig. 8(a). By combining the information we can conclude that the quantity of hydrogen bonds between DNA and water decreases as the concentration increases. To gain deeper insights into the molecular interactions governing these conformational changes, we further analyzed the hydrogen bonding patterns between DNA and ethanol molecules, which are presented in Fig. 8(b).

The quantitative analysis reveals a distinct correlation between ethanol concentration and hydrogen bonding patterns: while the number of DNA–ethanol hydrogen bonds exhibits a positive correlation with increasing ethanol concentration, the DNA–water hydrogen bonding shows an inverse relationship. This observation can be attributed to ethanol's dual molecular effects: direct disruption of the DNA's hydrogen bonding network, and indirect long-range effects through modification of the solution's dielectric properties. Consequently, it can be concluded that an increase in concentration of ethanol solution can impede the formation of hydrogen bonds between DNA and water to some extent, leading to a reduction in the hydration of DNA molecules. This reduction in hydration facilitates the entry of Na^+ ions into the solvated shell surrounding the DNA phosphate group and their interaction with the DNA chain, ultimately promoting the conversion of B-DNA to A-DNA configuration. This finding is in agreement with the previous literature.[43]

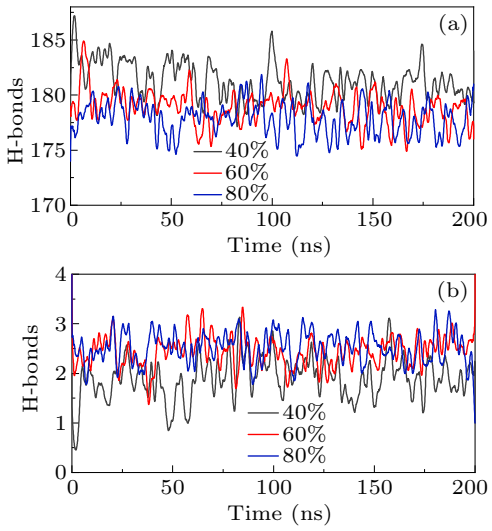


Fig. 8. (a) Hydrogen bonds between DNA and water molecules and (b) hydrogen bonds between DNA and ethanol molecules.

3.3. Radial distribution function

The radial distribution function (RDF) is a powerful tool for describing molecular microstructural changes, as it shows

how the density of matter varies as a function of distance from a reference point.[44] To understand the molecular mechanism underlying the concentration-dependent B-DNA to A-DNA transition at lower temperatures, we performed a detailed analysis of RDFs for both water oxygen atoms and Na^+ ions relative to the electronegative oxygen atoms in DNA phosphate groups, as presented in Fig. 9. It can be indicated from Fig. 9(a) that the first peak of the oxygen atoms in water is taller and narrower, indicating the formation of the first solvation shell around the phosphate group. It can be illustrated from Fig. 9(b) that Na^+ ions exhibit a preference for distributing within a range of 0.22–0.26 nm from the phosphate group, characterized by a notably high intensity. The radial distance of the first peak of the RDFs of Na^+ and water is very close, approximately 0.22–0.28 nm, indicating that the distribution of Na^+ nearly overlaps with the first solvation layer around the DNA phosphate group. As the concentration of ethanol increases, the first peak of the RDFs of Na^+ becomes higher and higher, indicating a higher density of Na^+ surrounding the phosphate group. This increase in density of both water and Na^+ around the phosphate group leads to a gradual increase in the electrostatic interaction between Na^+ and the phosphate group. Furthermore, higher ethanol concentrations substantially reduce DNA-water hydrogen bonding, leading to partial dehydration of the DNA structure.[45] This dehydration effect facilitates Na^+ ion penetration into the solvation shell surrounding the phosphate groups, enabling stronger ionic interactions with the DNA backbone. The combined effects of reduced water molecule mobility in the major groove and backbone regions, coupled with the increased cation migration toward the DNA backbone at elevated ethanol concentrations, ultimately drive the structural transition from B-DNA to A-DNA configuration.

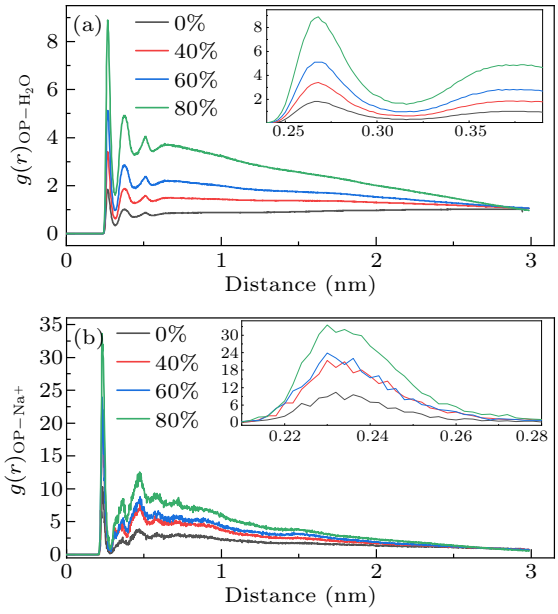


Fig. 9. (a) The RDFs of water oxygen atoms and (b) Na^+ ions around electronegative oxygen atoms of phosphate groups.

4. Conclusion

In this work, the concentration-dependent conformational transitions of 1ZEW in ethanol-water mixtures were systematically investigated through molecular dynamics simulations. Based on the simulation data, several conclusions can be drawn. At lower temperatures (below 300 K), higher concentrations of ethanol favor transitions from B-DNA to A-DNA. The primary mechanism underlying the transition from B-DNA to A-DNA is predominantly associated with the capacity of ethanol to diminish water activity, which hinders the formation of hydrogen bond between DNA and water molecules thereby weakening hydration effects and facilitates Na^+ ions' entry into the solvation shell surrounding the DNA phosphate groups. This interaction ultimately promotes Na^+ binding with the DNA chain and leads to its transformation from B-DNA to A-DNA. At the same time, at higher temperatures (above 320 K), a lower concentration facilitates the conformational transition from B-DNA to A-DNA. However, our structural analysis suggests that this temperature-induced transition involves more complex mechanisms beyond a simple B-DNA to A-DNA transformation. Through detailed characterization of the thermal denaturation profile, we determined the melting temperature of 1ZEW to be approximately 323.8 K. The observed structural changes at 320 K can be attributed to the onset of thermal melting, which accounts for the inverse trend observed in DNA structural parameters at this specific temperature regime.

Based on the systematic investigation conducted in this study, we have gained significant insights into the mechanistic relationship between solution microenvironment and DNA conformational dynamics, providing a fundamental understanding of environmental factors governing nucleic acid structural transitions. As the transition between A-DNA and B-DNA configurations represents a highly complex biological process involving intricate molecular interactions, continued research is needed to fully understand the mechanisms involved so that we can have a better understanding of how solution environment affects DNA configuration.

Acknowledgements

Project supported by the National Natural Science Foundation of China (Grant Nos. 52073128 and 11964012) and the Foundation of Educational Committee of Jiangxi Province of China (Grant No. GJJ2201314).

References

[1] Mukherjee S K, Gautam S, Biswas S, Kundu J and Chowdhury P K 2015 *J. Phys. Chem. B* **119** 14145
[2] Sarkar M, Li C and Pielak G J 2013 *Biophys. Rev.* **5** 187
[3] Buldyrev S, Goldberger A, Havlin S, Mantegna R, Matsa M, Peng C K, Simons M and Stanley H 1995 *Phys. Rev. E* **51** 5084

[4] Richter K, Nessling M and Lichter P 2007 *J. Cell. Sci.* **120** 1673
[5] Richter K, Nessling M and Lichter P 2008 *BBA Mol. Cell Res.* **1783** 2100
[6] Akabayov B and Richardson C C 2012 *Biophys. J.* **102** 281
[7] Norred S E, Caveney P M, Chauhan G, Collier L K, Collier C P, Abel S M and Simpson M L 2018 *ACS Synth. Biol.* **7** 1251
[8] Kong J W, Dou S X, Li W, Li H and Wang P Y 2023 *Chin. Phys. Lett.* **40** 078701
[9] Zhang S H, Niu X Z, Wang X Z, Qu C, An H L, Zhao T J and Zhan Y 2023 *Chin. Phys. B* **32** 050504
[10] Putzel G G, Tagliazucchi M and Szleifer I 2014 *Phys. Rev. Lett.* **113** 138302
[11] Wang F, Baquero D P, Beltran L C, Su Z, Osinski T, Zheng W, Prangishvili D, Krupovic M and Egelman E H 2020 *Proc. Natl. Acad. Sci. USA* **117** 19643
[12] Castaneda N, Lee M, Rivera-Jacquez H J, Marracino R R, Merlino T R and Kang H 2019 *J. Phys. Chem. B* **123** 2770
[13] Lai C T and Schatz G C 2018 *J. Phys. Chem. B* **122** 7990
[14] Yao F, Peng X, Su Z, Tian L, Guo Y and Kang X f 2020 *Anal. Chem.* **92** 3827
[15] Ghosh S, Takahashi S, Ohyama T, Endoh T, Tateishi-Karimata H and Sugimoto N 2020 *Proc. Natl. Acad. Sci. USA* **117** 14194
[16] Shet S M, Bharadwaj P, Bisht M, Pereira M M, Thayallath S K, Lokesh V, Franklin G, Kotrappanavar N S and Mondal D 2022 *Int. J. Biol. Macromol.* **215** 184
[17] Deng Z, Prem C and Fenfei L 2023 *J. Biol. Chem.* **299** 105439
[18] Kumar J A, Rakesh S, Preeti P and Pradipta B 2018 *Plos One* **13** e0206359
[19] Zhang N, Li M R, Xu H T and Zhang F S 2020 *Chin. Phys. Lett.* **37** 088701
[20] Shim A R, Nap R J, Huang K, Almassalha L M, Matusda H, Backman V and Szleifer I 2020 *Biophys. J.* **118** 2117
[21] Khoshbin Z, Housaindokht M R, Izadyar M, Bozorgmehr M R and Verdian A 2020 *Mol. Simul.* **46** 592
[22] Hong F, Schreck J S and Šulc P 2020 *Nucleic Acids Res.* **48** 10726
[23] Xue J J, Li X P, Tan R R and Zong W J 2022 *Chin. Phys. B* **31** 048702
[24] Xue J, Wang P, Li X, Tan R and Zong W 2022 *Biophys. Chem.* **288** 106845
[25] Hays F A, Teegarden A, Jones Z J, Harms M, Raup D, Watson J, Cavaliere E and Ho P S 2005 *Proc. Natl. Acad. Sci. USA* **102** 7157
[26] Li J, Xie S, Zhang B, He W, Zhang Y, Wang J and Yang L 2024 *Crit. Rev. Eukaryot. Gene. Expr.* **34** 11
[27] Mondal S, Mondal T K, Rajesh Y, Mandal M and Sinha C 2018 *Polyhedron* **151** 344
[28] Mark P and Nilsson L 2002 *J. Phys. Chem. B* **106** 9440
[29] Berendsen H J, Grigera J R and Straatsma T P 1987 *J. Phys. Chem. C* **91** 6269
[30] Abraham M J, Murtola T, Schulz R, Páll S, Smith J C, Hess B and Lindahl E 2015 *Softw. X* **1–2** 19
[31] Lindorff-Larsen K, Piana S, Palmo K, Maragakis P, Klepeis J L, Dror R O and Shaw D E 2010 *Proteins* **78** 1950
[32] Darden T, York D and Pedersen L 1993 *J. Chem. Phys.* **99** 10089
[33] Lavery R, Moakher M, Maddocks J H, Petkeviciute D and Zakrzewska K 2009 *Nucleic Acids Res.* **37** 5917
[34] Li S, Olson W K and Lu X J 2019 *Nucleic Acids Res.* **47** W26
[35] Markham N R and Zuker M 2005 *Nucleic Acids Res.* **33** W577
[36] Calladine C 1982 *J. Mol. Biol.* **161** 343
[37] Stofer E and Lavery R 1994 *Biopolymers* **34** 337
[38] El Hassan M and Calladine C 1998 *J. Mol. Biol.* **282** 331
[39] Zhang H, Fu H, Shao X, Dehez F, Chipot C and Cai W 2019 *J. Chem. Inf. Model.* **59** 2324
[40] Messelson M 1958 *Proc. Natl. Acad. Sci. USA* **44** 671
[41] Mergny J L and Lacroix L 2003 *Oligonucleotides* **13** 515
[42] Steiner T 2002 *Angew. Chem. Int. Ed.* **41** 48
[43] Tolokh I S, Pabit S A, Katz A M, Chen Y, Drozdetski A, Baker N, Pollack L and Onufriev A V 2014 *Nucleic Acids Res.* **42** 10823
[44] Kirkwood J G and Boggs E M 1942 *J. Chem. Phys.* **10** 394
[45] Wu Y Y, Zhang Z L, Zhang J S, Zhu X L and Tan Z J 2015 *Nucleic Acids Res.* **43** 6156